



RESEARCH ARTICLE

Cite this: *RSC Med. Chem.*, 2023, 14, 692Design, synthesis and evaluation of the anti-breast cancer activity of 1,3-oxazolo[4,5-*d*]pyrimidine and 1,3-oxazolo[5,4-*d*]pyrimidine derivatives†Yevheniia Velihina, ^{*ab} Raey Gesese,^c Victor Zhirnov,^a Oleksandr Kobzar,^d Benjamin Bui,^c Stepan Pilyo,^a Andriy Vovk,^d Hai-Ying Shen ^c and Volodymyr Brovarets^{*a}

A series of 1,3-oxazolo[4,5-*d*]pyrimidine and 1,3-oxazolo[5,4-*d*]pyrimidine derivatives were synthesized and functionalized in this study. The obtained compounds were tested against breast cancer cell lines of the NCI subpanel, followed by further analysis using the COMPARE algorithm from the Therapeutics Development Program, NCI. All synthesized derivatives displayed activity against most cell lines in the range of micromolar concentrations in terms of all parameters studied. Oxazolopyrimidine **5** exhibited the highest antitumor activity. A standard COMPARE analysis of the compounds showed that the vectors of the cytotoxic activity of derivatives **10** and **11** displayed a close to very high correlation with tamoxifen, and oxazolopyrimidine **13** displayed a very high correlation with the same drug. Five derivatives (**2**, **4**, **6**, **11** and **13**) showed a high correlation with aclacinomycin A in the TGI vector. At the same time, compound **1** effectively suppressed ADK in cultured MDA-MB 231 cell lines, indicating that ADK is one of its targets through which it exerts anticancer properties. Based on molecular docking results, the possible binding mode of oxazolopyrimidine **1** to ADK has been suggested.

Received 14th October 2022,
Accepted 14th February 2023

DOI: 10.1039/d2md00377e

rsc.li/medchem

Introduction

Breast cancer is the most commonly diagnosed cancer and the leading cause of cancer death among women worldwide.^{1,2} It accounted for 25.5% of the total number of cancer cases diagnosed in 2020, and death was observed in a third of cases. While chemotherapy and neoadjuvant therapy are important approaches practiced in addition to surgical treatment, breast cancer patients are compromised by high mortality and morbidity, as well as the ineffectiveness of existing drugs. These are the basis for the search for new compounds with *in vitro* antitumor activity for the development of new antitumor drugs that are effective *in vivo*.

The derivatives of 1,3-oxazole containing nitrogen and oxygen atoms in positions **1** and **3** of the five-membered

heterocycle, respectively, can bind to various enzymes and cell receptors through non-covalent interactions, which elicit their biological activity. Moreover, functionalizing them with various pharmacophores provides a rational design approach for the development of new anticancer drugs. So far, the synthesized 1,3-oxazole derivatives have shown high anticancer activity through interactions with various cellular targets, resulting in both delayed proliferation and the death of cancer cells.^{3–6} Taken together, 1,3-oxazole holds a promising background for the development of new drugs against cancer cells.

In this study, we aimed to evaluate some synthesized 1,3-oxazolo[4,5-*d*]pyrimidine and 1,3-oxazolo[5,4-*d*]pyrimidine derivatives in treating breast cancer cells. We have demonstrated our findings from *in vitro* studies on the NCI subpanel activity of 14 synthesized compounds against breast cancer cell lines.

Results and discussion

The synthesis of target oxazolopyrimidine derivatives

The synthesis of 1,3-oxazolo[4,5-*d*]pyrimidine and 1,3-oxazolo[5,4-*d*]pyrimidine derivatives **1–14** was accomplished using previously developed approaches,⁷ as depicted in Schemes 1 and 2. Compounds **1–12** were obtained by a sequence of reactions starting from available

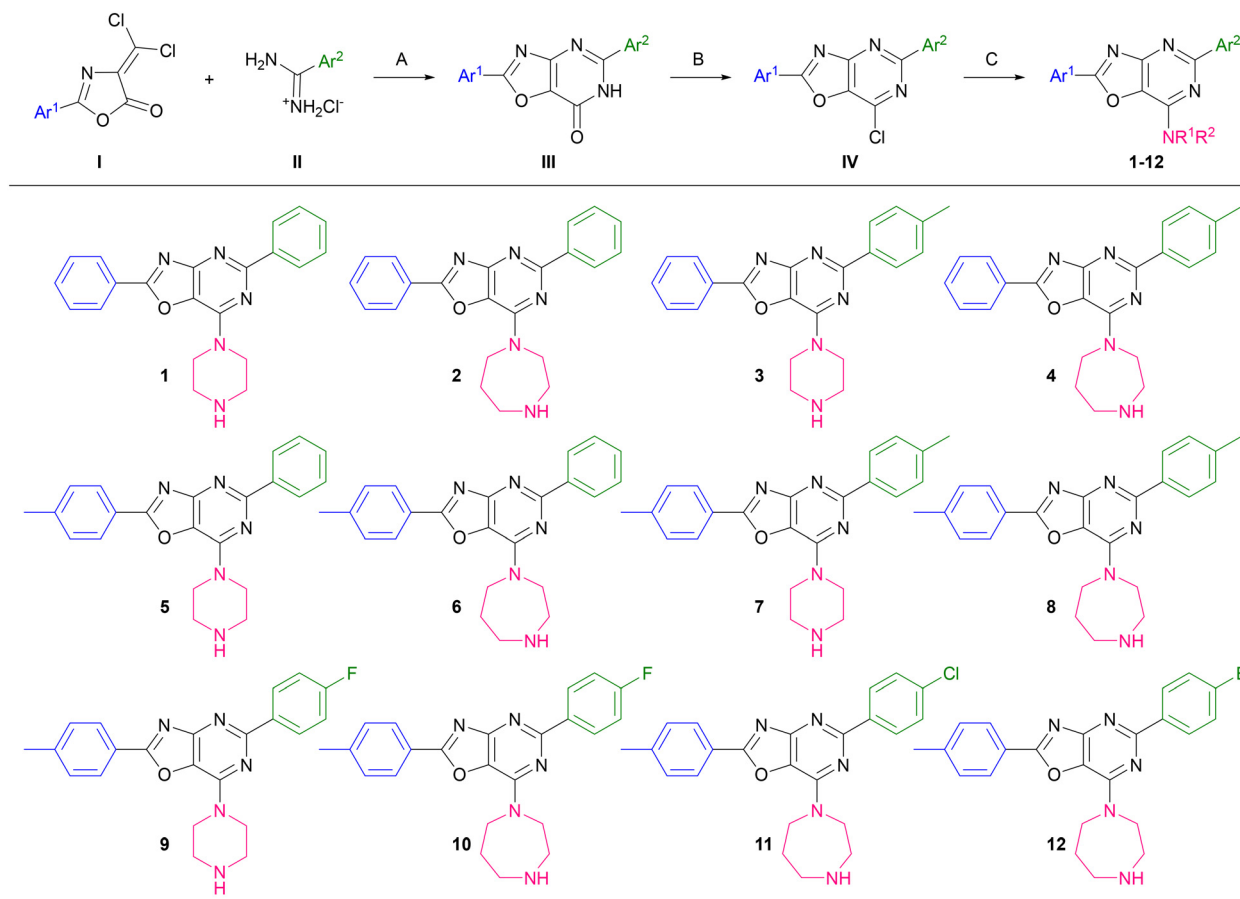
^a Department of Chemistry of Bioactive Nitrogen-Containing Heterocyclic Bases, V. P. Kukhar Institute of Bioorganic Chemistry and Petrochemistry, NAS of Ukraine, Kyiv, 02094, Ukraine. E-mail: brovarets@bpci.kiev.ua

^b Laboratoire COBRA, INSA Rouen Normandie, Bâtiment IRCOF, rue Tesnière 1, Mont Saint-Aignan Cedex, 76821, France. E-mail: yevheniia.velihina@insa-rouen.fr

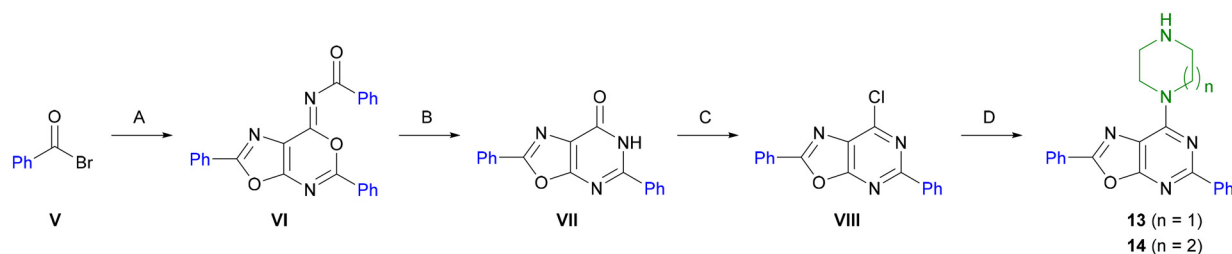
^c RS Dow Laboratories, Legacy Research Institute, Legacy Health, 1225 NE 2nd Ave, Portland, OR 97232, USA

^d Department of Bioorganic Mechanisms, V.P. Kukhar Institute of Bioorganic Chemistry and Petrochemistry, NAS of Ukraine, Kyiv, 02094, Ukraine

† Electronic supplementary information (ESI) available. See DOI: <https://doi.org/10.1039/d2md00377e>



Scheme 1 Reagents and conditions: (A) TEA, THF, r.t., 48 h; then Py, reflux, 10 h; (B) POCl₃, Me₂NPh, reflux, 3 h; (C) amine, TEA, dioxane, reflux, 6 h; see the Experimental section for yields.



Scheme 2 Reagents and conditions: (A) AgCN, THF, reflux, 21 h; (B) MeONa, MeOH, r.t. 16 h; then AcOH, r.t. 1 h; (C) POCl₃, Me₂NPh, reflux, 3 h; (D) amine, TEA, dioxane, reflux, 6 h; see the Experimental section for yields.

2-aryl-4-dichloromethylene-1,3-oxazol-5(4*H*)-one **I**.⁸ Treating **I** with amidine hydrochlorides **II** in the presence of triethylamine followed by heating in the presence of pyridine afforded the cyclo-condensation products **III**.

The reaction of compounds **III** with trichloro phosphate in the presence of *N,N*-dimethylaniline afforded 2,5-diaryl-7-chloro-1,3-oxazolo[4,5-*d*]pyrimidines **IV**. Derivatives **IV** were then converted to desired 7-amine-substituted 1,3-oxazolo[4,5-*d*]pyrimidines **1–12** by a reaction with piperazine or diazepam. The structures of the intermediates **III** and **IV** have been reliably established earlier.⁹ The ¹H-

NMR spectra of **1**, **3**, **5** and **7** in (D₆)-DMSO revealed a singlet at 2.30–2.43 ppm due to the NH-piperazine moiety, and the signal of the NH proton in the 1,4-diazepane moiety of **2**, **4**, **6** and **8–12** was not observed.

Isomeric 1,3-oxazolo[5,4-*d*]pyrimidin-7-one **VII** was synthesized using the previously described route (Scheme 2).⁷ The reaction of benzoyl bromide **V** with silver cyanide led to the formation of oxazolo[3,4-*d*][1,3]oxazine **VI**. The treatment of the **VI** trimer with sodium methoxide followed by stirring with acetic acid afforded 2,5-diphenyl-oxazolo[5,4-*d*]pyrimidin-7-one **VII**.

The reaction of compound **VII** with trichloro phosphate in the presence of *N,N*-dimethylaniline yielded 2,5-diphenyl-7-chlor-1,3-oxazolo[5,4-*d*]pyrimidine **VIII**. Derivative **VIII** was converted to the desired 7-amine-substituted 1,3-oxazolo[5,4-*d*]pyrimidines **13** and **14** by its reaction with piperazine or diazepam.

One-dose assay

According to the sensitivity of the tested cell lines to the series of synthesized derivatives, they could be arranged in the following order: MDA-MB-231 (176 ± 5) > MCF7 (169 ± 3) > T-47D (139 ± 8) > HS 578T (103 ± 17) > BT-549 (55 ± 19). Although this range is of no practical importance, to some extent, it allowed us to evaluate the overall antitumor activity of the synthesized series of compounds against individual cell lines. It should be noted that all derivatives showed pronounced cytotoxic activity against the MCF7, MDA-MB-231, MDA-MB-468, and T-47D cell lines, except for compound **9**, which weakly suppressed the MDA-MB-468 line, as well as compounds **7** and **14**, which showed little activity against T-47D. The least sensitive lines were BT-549 and HS 578T, which were insensitive to compounds **3**, **4**, **7**, **9**, and **11–14**, and **3**, **7**, **8**, **13**, and **14**, respectively.

The tested breast cancer lines belonged to subtypes with different immune profiles and molecular characteristics: luminal A (MCF-7 and T47D), basal (MDA-MB-468), and claudin-low (BT549, MDA-MB-231, and Hs578T) subtypes. For example, MCF7 and T-47D are endocrine-responsive lines that express estrogen (ER) and progesterone receptors (PR). In contrast, MDA-MB-468 is an endocrine-nonresponsive line that expresses EGFR and/or cytokeratin 5/6, while BT549, MDA-MB-231 and, Hs578T lack ER, PR and human epidermal growth factor receptor 2 (HER2).^{10,11} Despite these molecular differences, compounds **5** and **10** showed pronounced cytotoxicity against all tested lines, regardless of the immune profile.

Individual compounds also showed differences in breast cancer cell sensitivity. According to the average values of the degree of inhibition of cell growth, the synthesized compounds could be arranged in the following order (the percentage of inhibition is indicated in brackets): **10** (175) ≈ **5** (171) > **1** (155) > **6** (145) ≈ **2** (144) ≈ **4** (143) > **11** (133) > **12** (123) ≈ **3** (122) > **13** (110) > **8** (99) ≈ **9** (97) ≈ **7** (93) > **14** (83). The first two compounds equally and actively suppressed all cell lines of the sub-panel. Compounds **1** and **2** showed a similar low-selective effect, but they were somewhat inferior to the preceding ones in terms of the average activity value. Moreover, the antitumor activity of compound **1**, unlike **2**, did not significantly differ from those of **5** and **10**. Thus, according to the results of the one-dose analysis, among the tested compounds, derivatives **10**, **5**, and **1** showed the highest activity against all cell lines of the breast cancer NCI subpanel (see Table 1).

Five-dose assay

Table 2 shows the results of a five-dose assay of the synthesized compounds. These data indicate the high antitumor activity of the synthesized 1,3-oxazole derivatives against most cell lines in the NCI breast cancer subpanel. Furthermore, the statistical analysis of these data showed that, depending on the analyzed parameter, the compounds could be organized in certain activity series.

According to the average concentration of the entire subpanel needed for the growth inhibition (GI₅₀) of cell lines, the compounds ranked in the following series (μM): **5** (0.8) > **10** (1.6) = **2** (1.6) > **6** (1.7) = **4** (1.7) > **1** (1.8) = **13** (1.8) > **11** (1.9) > **7** (3.5) > **12** (7.3), and according to the statistical significance of the differences, the order was: **5** (0.8 ± 0.33) > **14** (1.2 ± 0.58) = **10** (1.6 ± 0.09) = **2** (1.6 ± 0.07) = **6** (1.7 ± 0.06) = **4** (1.7 ± 0.08) = **1** (1.8 ± 0.08) = **13** (1.8 ± 0.05) = **11** (1.9 ± 0.04) > **7** (3.5 ± 1.58) = **9** (3.9 ± 1.95) = **3** (3.9 ± 1.98) = **8** (6.1 ± 2.70) = **12** (7.3 ± 2.96). Thus, for most compounds, the GI₅₀

Table 1 Data from the antitumor screening of the synthesized compounds against human breast cancer cell lines in the one-dose assay

Compound	NSC number	MCF7	MDA-MB-231	HS 578T	BT-549	T-47D	MDA-MB-468	Mean ± SEM
1	811 837	162	187	161	106	142	174	155 ± 12
2	762 211	132	180	131	126	123	171	144 ± 10
3	802 770	175	179	72	15	158	131	122 ± 27
4	802 771	175	192	130	19	167	176	143 ± 26
5	802 769	166	179	151	172	168	187	171 ± 5
6	802 774	178	187	118	72	145	168	145 ± 18
7	802 772	173	172	1	17	63	133	93 ± 31
8	802 773	165	179	0	10	146	95	99 ± 32
9	821 725	174	129	106	1	127	46	97 ± 26
10	821 726	172	185	176	177	164	176	175 ± 3
11	821 727	179	176	151	1	136	154	133 ± 27
12	821 728	176	157	130	1	108	165	123 ± 26
13	818 706	169	181	11	3	157	137	110 ± 33
14	818 707	167	103	16	5	53	153	83 ± 28

Notes: The compounds were added at a concentration of 1×10^{-5} M, and the culture was incubated for 48 h. The numbers reported represent growth inhibition (%) in the one-dose assay relative to the no-drug control and relative to the time-zero number of cells. This setting allows for the detection of growth inhibition (values between 0 and 100) and lethality (values more than 100). A value of 200 means all cells were dead.

Table 2 Parameters associated with the anticancer activity of the tested compounds against breast cancer cell lines in the five-dose assay

Compound	Cell line																	
	MCF7			MDA-MB-231			HS 578T			BT-549			T-47D			MDA-MB-468		
	GI ₅₀	TGI	LC ₅₀	GI ₅₀	TGI	LC ₅₀	GI ₅₀	TGI	LC ₅₀	GI ₅₀	TGI	LC ₅₀	GI ₅₀	TGI	LC ₅₀	GI ₅₀	TGI	LC ₅₀
1	1.48	3.31	7.40	1.76	3.28	6.10	1.88	4.07	8.80	1.77	3.41	—	2.10	4.95	>100	1.73	3.42	—
2	1.41	2.83	5.69	1.56	2.97	5.65	1.86	4.13	9.16	1.73	3.18	5.86	1.69	3.48	7.15	1.48	2.87	5.54
3	1.85	3.75	7.60	1.62	3.06	5.77	2.53	7.69	>100	13.8	31.6	72.7	1.81	3.83	8.07	1.81	3.80	7.98
4	1.59	3.44	7.45	1.77	3.27	6.06	1.94	4.22	9.21	1.62	3.14	—	2.02	4.00	7.94	1.55	3.24	6.75
5	0.33	1.45	5.74	0.26	0.67	2.61	2.02	4.22	—	1.72	3.20	5.99	0.35	1.51	6.33	0.29	1.18	4.84
6	1.48	3.50	8.29	1.81	3.32	6.10	1.83	4.02	8.85	1.63	3.19	6.25	1.72	3.50	7.10	1.59	3.35	7.04
7	1.72	3.68	7.86	1.74	3.44	6.81	2.27	5.83	>100	1.71	3.32	6.48	11.4	37.35	>100	2.13	4.77	13.50
8	1.85	3.88	8.14	1.69	3.11	5.73	12.6	31.9	80.9	16.3	35.0	75.2	1.94	4.17	8.96	1.96	4.39	—
9	1.66	3.51	7.40	1.86	3.63	7.09	2.06	5.12	37.0	13.6	30.1	66.8	2.30	6.92	>100	1.74	3.38	6.56
10	1.23	2.96	7.14	1.63	3.11	5.91	1.78	3.69	7.63	1.66	3.37	6.85	1.85	3.94	—	1.58	3.18	6.41
11	1.70	3.39	6.75	1.87	3.37	6.21	1.93	4.17	9.02	1.90	3.61	6.86	1.94	4.14	8.84	1.78	3.42	6.59
12	1.78	3.51	6.91	1.93	4.05	8.50	17.2	37.1	80.2	16.0	34.6	75.0	3.06	13.90	65.5	3.98	15.9	52.50
13	1.70	3.58	7.54	1.67	3.20	6.13	1.87	4.11	9.05	1.67	3.24	6.27	1.94	4.19	—	1.93	3.66	6.94
14	1.67	3.34	6.67	1.72	3.21	5.99	1.86	3.94	8.34	1.78	3.29	—	1.78	3.64	7.42	1.72	3.37	6.57

Notes: GI₅₀ – 50% growth inhibition, TGI – total growth inhibition (cytostatic effect) and LC₅₀ – 50% lethality (cytotoxic effect). The data are expressed in μM.

values were in the range of 1–2 μM, and for 3, 7, 8, 9 and 12, the range was 4–7 μM.

According to statistically significant differences in cytostatic activity (TGI), the compounds could be arranged as follows: 5 (2.04 ± 0.56) > 2 (3.24 ± 0.2) = 10 (3.38 ± 0.15) = 14 (3.46 ± 0.11) = 6 (3.48 ± 0.12) = 4 (3.55 ± 0.18) = 13 (3.66 ± 0.17) = 11 (3.68 ± 0.15) = 1 (3.74 ± 0.27) > 9 (8.78 ± 4.30) = 3 (8.96 ± 4.58) = 7 (9.73 ± 5.54) = 8 (13.74 ± 6.25) = 12 (18.18 ± 5.96). As in the previous case, the cytostatic concentration of compounds 3, 7, 8, 9 and 12 (9–18 μM) exceeded those (2–4 μM) of other derivatives.

Compounds 1, 3 and 7 were excluded from the statistical analysis of cytotoxic activity (LC₅₀) due to the presence of undefined values (LC₅₀ > 100 μM) or incomplete data. The remaining compounds were arranged according to the average value of cytotoxic concentration (μM) as follows: 5 (5.1) > 2 (6.5) > 10 (6.8) > 14 (7.0) > 13 (7.2) > 6 (7.3) > 11 (7.4) > 4 (7.6) > 9 (25.0) > 8 (35.8) > 12 (48.1). Moreover, the cytotoxicity of compound 5 (5.10 ± 0.67) in this series was significantly higher than those of the other compounds. Again, the cytotoxicity of compounds 8, 9 and 12 (LC₅₀ = 25–48 μM) was significantly lower than those of the other compounds (LC₅₀ = 5–7 μM).

The ranking of the antiproliferative activity of the compounds (GI₅₀ and TGI parameters), calculated as the ratio of the sum of occupied places in the rows of activity to their number (shown in parentheses), looked like: 5 (1) > 2 (3) = 10 (3) = 14 (3) > 6 (5) > 4 (6) > 13 (7.5) > 1 (9.5) = 11 (9.5) > 9 (10.5) > 7 (11) > 3 (11.5) > 8 (13) > 12 (14). The same order was also observed for the first four compounds in terms of the cytotoxicity parameter. Therefore, in all respects, compound 5 was the most effective against the tested human breast cancer cell lines, and the antitumor efficacies of 2, 10 and 14 were inferior to the former but exceeded those of the other compounds.

From the above statistical analysis, it is evident that any functional modification of the structure of compound 5 would lead to a decrease in all its antitumor activity parameters, whereas compounds 1, 2, 4, 6, 11, 13 and 14 are equally effective regardless of the substituents used in the oxazolo[4,5-*d*]pyrimidine backbone. On the other hand, the replacement of 1,4-diazepane at position 7 of compound 4 with piperazine (3) more than halved its antiproliferative activity and cytotoxicity. The replacement of the phenyl radical in the 2nd position of compound 4 with the 4-methylphenyl group (8) and the bromination of the phenyl residue (12) in the fifth position of compound 6, led to a similar result. The same pattern was observed with the fluorination (compound 9) or methylation (7) of the phenyl substituent in the fifth position of compound 5.

COMPARE correlations

Standard COMPARE analyses were performed on all tested parameters with antineoplastic agents of a known mode of action as standards. The following scale of interpretation of the pair correlation coefficients was used: insignificant (0.00–0.30), weak (0.30–0.50), moderate (0.50–0.70), high (0.70–0.90), and very high (0.9–1.0).¹²

The COMPARE matrix using the GI₅₀ vector showed a high positive correlation for compounds 2, 6 and 13 with CCNU and 11 with methyl-CCNU, which performs major-groove-directed DNA alkylation at guanine residues (see Table 3). It also carbamoylates DNA and proteins, resulting in the inhibition of DNA and RNA synthesis and disruption of RNA processing.¹³ Compounds 5 and 12 showed a high positive correlation with pyrazofurin (a nucleoside analog), which inhibits orotidine-5'-monophosphate decarboxylase, thereby interfering with *de novo* uridine nucleotide synthesis. This agent also causes a rapid depletion of the pyrimidine

Table 3 Standard agent COMPARE correlations for the synthesized compounds

Compound	GI ₅₀	TGI	LC ₅₀
1	CCNU (0.62)	Actinomycin D (0.63)	Dihydroleupone (0.53)
2	CCNU (0.84)	Aclacinomycin A (0.82)	Caracemide (0.65)
3	Tiazofurin and pyrazofurin (0.45)	CCNU (0.34)	Caracemide (0.40)
4	CCNU (0.67)	Aclacinomycin A (0.73)	Caracemide (0.46)
5	Pyrazofurin (0.71)	Macbecin II (0.46)	CHIP (0.52)
6	CCNU (0.71)	Aclacinomycin A (0.88)	Caracemide (0.53)
7	Cyclopentenyl-cytosine (0.65)	L-Cysteine analogue (0.48)	Rifamycin SV (0.43)
8	Cyclopentenyl-cytosine (0.54)	CCNU (0.46)	Methyl-CCNU (0.32)
9	N,N-Dibenzyl-daunomycin (0.61)	Rifamycin SV (0.43)	Rifamycin SV (0.49)
10	Methyl-CCNU (0.65)	Caracemide (0.68)	Tamoxifen (0.74)
11	Methyl-CCNU (0.73)	Aclacinomycin A (0.82)	Tamoxifen (0.76)
12	Pyrazofurin (0.72)	N,N-Dibenzyl-daunomycin (0.45)	Hydrazine sulfate (0.41)
13	CCNU (0.84)	Aclacinomycin A (0.79)	Tamoxifen (0.91)
14	Actinomycin D (0.61)	Rapamycin (0.48)	Rapamycin (0.40)

deoxynucleotide pool, thereby inhibiting DNA synthesis and cell replication. Five compounds (**2**, **4**, **6**, **11** and **13**) showed a high correlation in the TGI vector with aclacinomycin A (aclerubicin), which intercalates into DNA, thereby inhibiting DNA replication and repair and RNA and protein synthesis,¹⁴ and interacts with topoisomerases **I** and **II**.¹⁵ It seems that their antiproliferative activity is largely due to direct interaction with the DNA of tumor cells. The antiproliferative action of compounds **5** and **12** may mechanistically include direct interaction with DNA and indirect influence through the inhibition of ornithine decarboxylase. Finally, the cytotoxic activity coefficients of compounds **10** and **11** were close to very high, and **13** had a very high correlation with tamoxifen, which is a selective estrogen receptor modulator that inhibits growth and promotes apoptosis in estrogen-receptor-positive tumors.¹⁶ It also exhibits ER-independent anticancer effects by disrupting the mitochondrial bioenergetic function and inducing cell apoptosis.¹⁷ This allows us to accept this mechanism of action as the leading route underlying the cytotoxic activity of these oxazole derivatives. The data obtained from the COMPARE analysis of some compounds are not included here due to weak or moderate correlation with the identified reference drugs or they did not provide sufficient evidence to identify the molecular targets underlying their cytotoxic activity.

The suppression of adenosine kinase on MB231 cells with compound 1

The weak or moderate correlations of most of the synthesized compounds (**1**, **3**, **5**, **7–10**, **12** and **14**) with standard preparations according to the TGI vector suggest that their cytostatic activity is through interaction with specific molecular targets. We hypothesized that adenosine kinase could be one of the most likely targets due to its high expression in breast cancer cells.¹⁸ Adenosine kinase (ADK; EC 2.7.1.20) is a ribokinase that exists in two isoforms: the cytoplasmic short isoform (ADK-S) and the nuclear long isoform (ADK-L). DNA methylation plays an important role in cancer development, and it is suggested that ADK-L

determines global DNA methylation in cancer cells and may be a potential therapeutic target to eliminate DNA hypermethylation in cancer.^{19,20} It has been shown that the ADK-L expression level is significantly increased in breast cancer tissues *versus* paired normal tissues adjacent to the tumor, whereas the ADK-S expression levels are not significantly different between cancerous and normal tissues. The inhibition of ADK isoforms leads to suppressed cellular proliferation, division, and migration of cultured breast cancer cells.¹⁸ Through this mechanism, ADK-L controls the adenosine-receptor-independent epigenetic function of adenosine.²¹ ADK-S regulates the intra- and extracellular levels of adenosine. High levels of ADK-S contribute to adenosine deficiency and decreased activation of adenosine receptors. It is assumed that the tumor avoids immune surveillance by reducing the level of ADK-S. Thus, ADK-L and ADK-S control the adenosine concentrations in different cellular compartments and play different roles in influencing cancer biology.²²

Compound **1**, which showed only moderate correlation with the standard drugs across all three characteristic vectors (GI₅₀, TGI, and LC₅₀), was chosen to study its effect on adenosine kinase in the breast cancer MDA-MB-231 cell line and those with genetically modified ADK isoform profiles, *i.e.*, MDA-ADK-L-KD and MDA-ADK-S-KD (Fig. 1).¹⁸

Further, using three established mutant MB231 cell lines, *i.e.*, ADK-L knockdown (L-KD) and ADK-S knockdown (S-KD), and non-modified wild-type (WT) MB231 cells, we tested the effect of oxazolopyrimidine **1** on proliferation in comparison with a conventional ADK inhibitor 5-ITU. The results showed that (i) in MB231-WT cells, compound **1** effectively suppressed proliferation *vs.* vehicle controls ($p < 0.0001$, $F_{(8,24)} = 25.82$, treatment \times time factors; $p < 0.0001$, $F_{(2,6)} = 173.1$, treatment factor; two-way ANOVA, $n = 6$ /treatment/time point) (Fig. 2A). This suppression effect of compound **1** was similar to 5-ITU treatment ($p < 0.0001$, $F_{(8,24)} = 53.14$, treatment \times time factors; $p < 0.0001$, $F_{(2,6)} = 124.7$, treatment factor; two-way ANOVA, $n = 6$ /treatment/time point) (Fig. 2B). Specifically, treatment with derivative **1** at 10 μ M effectively suppressed MB231-WT cell proliferation during the test

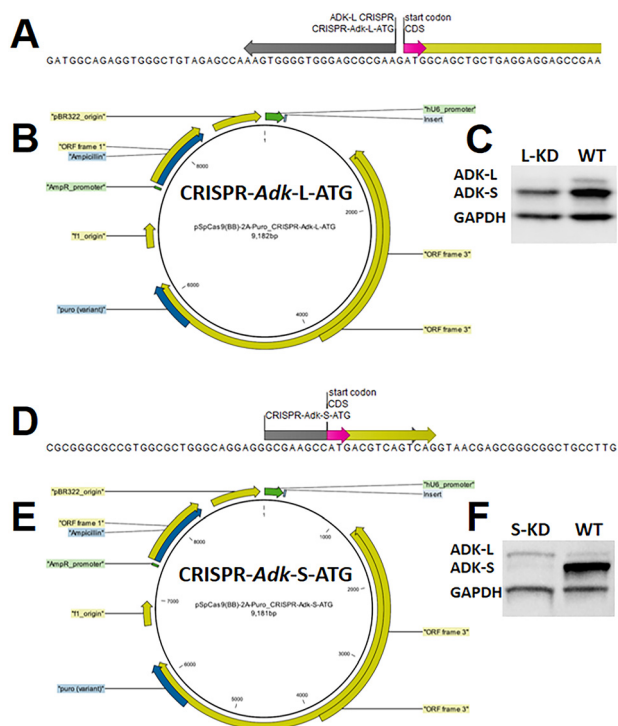


Fig. 1 CRISPR/Cas9-modified breast cancer MDA-MB-231 cells with altered ADK isoforms. (A and D) The schematic of the Adk gene is shown: the ADK-L and ADK-S start codons (in pink), ADK-S CRISPR binding region (in grey), and coding sequences (in yellow) are annotated. The plasmid maps of CRISPR/Cas9, with the gray-highlighted 'insert' label indicating the start codon of either (B) ADK-L or (E) ADK-S. (C and F) The representative image of Western blots of the ADK isoforms in breast cancer cells with or without ADK knockdown: MDA-ADK-L (L-KD), MDA-ADK-S (S-KD), and MDA-ADK-WT (WT) cells.

period from 24 h, 48 h, 72 h till 96 h (corresponding $p = 0.0017, 0.0075, 0.0021, \text{ and } 0.0003$, correspondingly, *post hoc* Dunnett test); compound **1** treatment at 3 μM also yielded effectively suppression of MB231-WT cells (Fig. 2A). (ii) In MDA231-S-KD cells, derivative **1** significantly suppressed proliferation *vs.* vehicle treatment ($p < 0.0001, F_{(8,24)} = 9.796$, treatment \times time factors; $p < 0.0001, F_{(2,6)} = 105.8$, treatment factor; two-way ANOVA, $n = 6/\text{treatment}/\text{timepoint}$) (Fig. 2A). However, two-way ANOVA analysis demonstrated better suppression of (S-KD) MDA231 cell growth with 5-ITU treatment ($p < 0.0001, F_{(8,24)} = 10.34$, treatment \times time factors; $p < 0.0001, F_{(2,6)} = 147.0$, treatment factor; two-way ANOVA, $n = 6/\text{treatment}/\text{time point}$), the cell suppression effect of ITU was observed even with a treatment dose of 3 μM at 48 h ($p = 0.0176$), 72 h ($p = 0.0474$), and 96 h ($p = 0.0002$), but was not seen at 1 μM ($p > 0.05$ for all timepoints, *post hoc* Dunnett test, $n = 6/\text{timepoint}$) (Fig. 2B). The data on MDA231-S-KD cells suggests the higher efficacy of oxazolopyrimidine **1** *vs.* 5-ITU with regard to antiproliferation. (iii) In MDA231-L-KD cells, compound **1** significantly suppressed growth *vs.* vehicle treatment ($p < 0.0001, F_{(8,24)} = 11.89$, treatment \times time factors; $p < 0.0001, F_{(2,6)} = 313.8$, treatment factor; two-way ANOVA, $n = 6/\text{treatment}/\text{timepoint}$); significant suppression was also

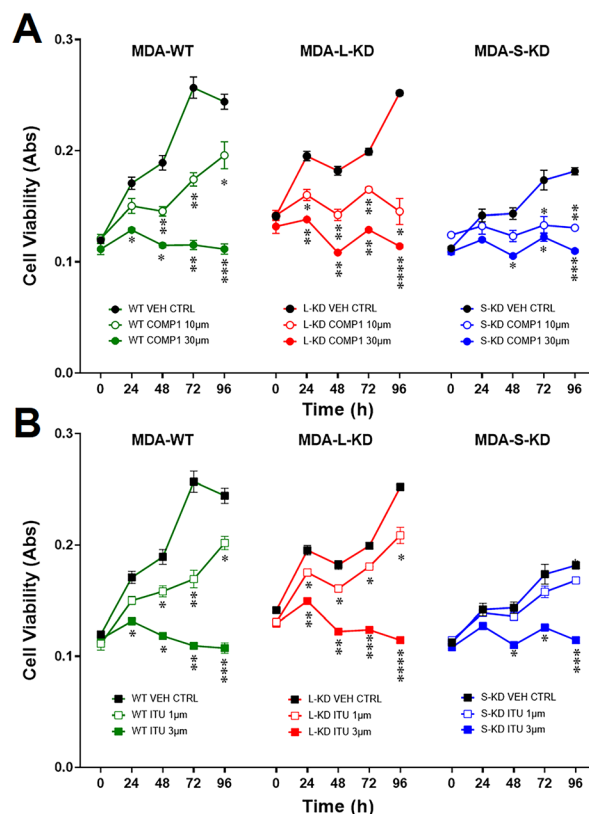


Fig. 2 The effect of compound **1** and 5-ITU on the proliferation of breast cancer cells. The effect of (A) compound **1** (COMP1) and (B) 5-ITU (ITU) treatments on the proliferation and cell viability of breast cancer cell lines: non-modified MDA-MB-231 (MDA-WT) cells and MDA-MB-231 cells with the knockdown of ADK-L (MDA-L-KD) and ADK-S (MDA-S-KD). Cell viability over time was quantified by the MTT assay ($n = 6/\text{treatment}/\text{timepoint}$). The measured formazan absorbance is considered directly proportional to the number of viable cells after treatment with COMP1 and ITU *vs.* vehicle controls (VEH CTRL). * $p < 0.05$; ** $p < 0.01$; *** $p < 0.001$; **** $p < 0.0001$ *vs.* corresponding VEH CTRL within the same cell line.

observed with 5-ITU treatment ($p < 0.0001, F_{(8,24)} = 52.46$, treatment \times time factors; $p < 0.0001, F_{(2,6)} = 776.4$, treatment factor; two-way ANOVA, $n = 6/\text{treatment}/\text{timepoint}$) (Fig. 2).

This dataset shows that oxazolo[4,5-*d*]pyrimidine **1** effectively suppressed ADK-containing WT/MB231 cells. Furthermore, it suppressed S-KD/MB231 and L-KD/MB231 cells, which have largely reduced levels of ADK isoforms, indicating its high selectivity and effect on ADK inhibition. Therefore, it can reasonably be assumed that one of the targets of compound **1**, given its antitumor activity at a concentration of 10 μM in the one-dose analysis, is ADK.

Molecular docking

Given the results of the *in vitro* experiments with compound **1** and ADK-containing MB-231 breast cancer cells, the 1,3-oxazolo[4,5-*d*]pyrimidine derivatives **1–12** and 1,3-oxazolo[5,4-*d*]pyrimidines **13** and **14** were docked into the

Table 4 Docking energies of the 1,3-oxazolo[4,5-*d*]pyrimidine and 1,3-oxazolo[5,4-*d*]pyrimidine derivatives **1–14** bound to the adenosine binding site of ADK

Compound	Affinity, kcal mol ⁻¹
1	-8.7
2	-8.8
3	-8.9
4	-9.2
5	-9.0
6	-9.5
7	-9.3
8	-9.5
9	-9.1
10	-9.7
11	-9.6
12	-9.4
13	-8.6
14	-8.8

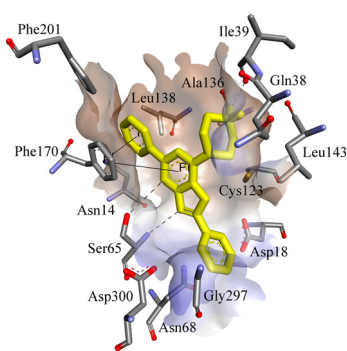


Fig. 3 The possible binding mode of compound **1** at the adenosine binding site of ADK.

adenosine binding site of adenosine kinase. The docking energies of all compounds were similar (Table 4), similar to their results in the anticancer studies. The molecular docking of compounds **1** and **5** revealed binding modes characterized by affinity values -8.7 kcal mol⁻¹ and -9.0 kcal mol⁻¹, respectively. In addition to electrostatic and van der Waals contacts, these models included a π - π -stacking interaction of the inhibitor with Phe170 and hydrogen bonds with Ile39 and Ser65 (Fig. 3).

Conclusions

1,3-Oxazole is a core structure in a wide variety of compounds with diverse biological and chemical applications and plays an important role in the drug discovery process. Twelve 1,3-oxazolo[4,5-*d*]pyrimidine derivatives and two new 1,3-oxazolo[5,4-*d*]pyrimidine derivatives were synthesized and their anti-breast cancer activity against cell lines in the NCI subpanel was evaluated *in vitro*. The bioassays showed that the synthesized compounds did display anti-breast cancer activity against most of the tested cancer cell lines. Among them, compound **5** (2-(4-methylphenyl)-5-phenyl-7-piperazin-1-yl-oxazolo[4,5-*d*]pyrimidine) exhibited the greatest

anticancer activity with $GI_{50} = 0.8 \pm 0.33$ μ M, $TGI = 2.04 \pm 0.56$ μ M and $IC_{50} = 5.10 \pm 0.67$ μ M. According to the results of the COMPARE analysis and *in vitro* experiments, adenosine kinase, topoisomerases **I** and **II**, and estrogen receptors may be the possible targets of the 1,3-oxazolo[4,5-*d*]pyrimidine and 1,3-oxazolo[5,4-*d*]pyrimidine derivatives. The data obtained allow us to consider oxazolopyrimidine as a promising backbone for the synthesis of new compounds with anti-breast cancer activity, as well as for the targeted search for new, highly effective drugs against breast cancer. Compound **5** can be studied in depth for antitumor activity both *in vitro* and *in vivo*.

Author contributions

The project and experiments were designed by Y. V., S. P., H.-Y. S., and V. B. The chemistry was performed by Ye. V. and S. P., the biological research was carried out by V. Zh., R. G., B. B., and H.-Y. S., and the computational work was conducted by O. K. and A. V. All authors contributed to the manuscript writing and review process.

Conflicts of interest

There are no conflicts to declare.

Acknowledgements

This work was supported by grants from the Good Samaritan Research Foundation of Legacy Health (No. 750390799, HYS). We would like to thank the US Public Health Service and the National Cancer Institute, Bethesda, MD, USA, for *in vitro* evaluation of anticancer activity (providing the NCI-60 cell testing) within the framework of the Developmental Therapeutic Program (<https://dtp.cancer.gov>) and Enamine Ltd for the material and technical support. Y. V. is grateful to INSA Rouen Normandie and the Région Normandie for financial support. The authors thank the experimental assistance from Tiffany B. Nguyen.

Notes and references

- D. J. van der Meer, I. Kramer, M. C. van Maaren, P. J. van Diest, S. C. Linn, J. H. Maduro, L. J. A. Strobbe, S. Siesling, M. K. Schmidt and A. C. Voogd, *Int. J. Cancer*, 2021, **148**, 2289–2303.
- S. Lei, R. Zheng, S. Zhang, S. Wang, R. Chen, K. Sun, H. Zeng, J. Zhou and W. Wei, *Cancer Commun.*, 2021, **41**, 1183–1194.
- X. Yan, J. Wen, L. Zhou, L. Fan, X. Wang and Z. Xu, *Curr. Top. Med. Chem.*, 2020, **20**, 1916–1937.
- N. Y. Guerrero-Pepinosa, M. C. Cardona-Trujillo, S. C. Garzon-Castano, L. A. Veloza and J. C. Sepulveda-Arias, *Biomed. Pharmacother.*, 2021, **138**, 111495.
- V. V. Zhirnov, Y. S. Velihina, O. P. Mitiukhin and V. S. Brovarets, *Chem. Biol. Drug Des.*, 2021, **98**, 561–581.

- 6 S. Kulkarni, K. Kaur and V. Jaitak, *Anti-Cancer Agents Med. Chem.*, 2022, **22**, 1859–1882.
- 7 Ye. Velihina, T. Scattolin, D. Bondar, S. Pil'ov, N. Obernikhina, O. Kachkovskiy, I. Semenyuta, I. Caligiuri, F. Rizzolio, V. Brovarets, Y. Karpichev and S. P. Nolan, *Helv. Chim. Acta*, 2020, **103**, e2000169.
- 8 B. S. Drach and G. N. Miskevich, *Russ. J. Org. Chem.*, 1974, **10**, 2315 (*Chem. Abstr.*, 1975, **82**, 72843).
- 9 V. M. Sviripa, A. A. Gakh, V. S. Brovarets, A. V. Gutov and B. S. Drach, *Synthesis*, 2006, **20**, 3462–3466.
- 10 D. L. Holliday and V. Speirs, *Breast Cancer Res.*, 2011, **13**, 215.
- 11 S. E. Smith, P. Mellor, A. K. Ward, S. Kendall, M. McDonald, F. S. Vizeacoumar, F. J. Vizeacoumar, S. Napper and D. H. Anderson, *Breast Cancer Res.*, 2017, **19**, 65.
- 12 M. M. Mukaka, *Malawi Med. J.*, 2012, **24**, 69–71.
- 13 S. Agarwal, D. Chadha and R. Mehrotra, *J. Biomol. Struct. Dyn.*, 2015, **33**, 1653–1668.
- 14 J. B. Chaires, J. E. Herrera and M. J. Waring, *Biochemistry*, 1990, **29**, 6145–6153.
- 15 N. Hajji, S. Mateos, N. Pastor, I. Dominguez and F. Cortes, *Mutat. Res.*, 2005, **583**, 26–35.
- 16 S. Lakshmi, A. Shanitha, D. Shiny, B. Rahul, R. Saikant, S. Sharaf, S. Abi and G. Rajmohan, *Current Research in Pharmacology and Drug Discovery*, 2022, **3**, 100080.
- 17 Y. Unten, M. Murai, T. Koshitaka, K. Kitao, O. Shirai, T. Masuya and H. Miyoshi, *Biochim. Biophys. Acta, Bioenerg.*, 2022, **1863**, 148520.
- 18 B. Shamloo, N. Kumar, R. H. Owen, J. Reemmer, J. Ost, R. S. Perkins and H. Y. Shen, *Oncotarget*, 2019, **10**, 7238–7250.
- 19 H. Y. Luo, H. Y. Shen, R. S. Perkins and Y. X. Wang, *Front. Pharmacol.*, 2022, **13**, 908882.
- 20 A. E. Wahba, D. Fedele, H. Gebri, E. AlHarfoush, K. S. Toti, K. A. Jacobson and D. Boison, *ACS Pharmacol. Transl. Sci.*, 2021, **4**, 680–686.
- 21 M. Murugan, D. Fedele, D. Millner, E. Alharfoush, G. Vegunta and D. Boison, *Neurochem. Int.*, 2021, **147**, 105054.
- 22 D. Boison, S. A. Masino, F. D. Lubin, K. Guo, T. Lusardi, R. Sanchez, D. N. Ruskin, J. Ohm, J. D. Geiger and J. Hur, *Sci. Rep.*, 2022, **12**, 380.